

000 001 002 003 004 005 006 007 008 009 010 011 012 013 014 015 016 017 018 019 020 021 022 023 024 025 026 027 028 029 030 031 032 033 034 035 036 037 038 039 040 041 042 043 044 045 046 047 048 049 050 051 052 053 CAN TRANSFORMERS REALLY DO IT ALL? ON THE COMPATIBILITY OF INDUCTIVE BIASES ACROSS TASKS

Anonymous authors

Paper under double-blind review

ABSTRACT

Transformers are remarkably versatile and their design is largely consistent across a variety of applications. But are they optimal for any given task or dataset? The answer may be key for pushing AI beyond the mere scaling of current designs.

Method. We present a method to optimize a transformer architecture for a given dataset, which we use as a tool to study optimal task-specific inductive biases. The method replaces the most important non-linearities (GeLUs, softmax) with components optimized on held out data. We then use each resulting new architecture with other datasets as a way to evaluate the compatibility between pairs of tasks.

Findings. On a range of popular algorithmic tasks, our method identifies new architectures with dramatic improvements in learning speed, generalization, and stability across seeds. These designs prove very task-specific, which means that the tasks require inductive biases very different from those of standard transformers. On a range of code and language modeling datasets, we also find architectures with consistent, yet smaller improvements. These designs now transfer much better across datasets, domains (English vs. computer code), and tokenizations.

Implications. These results show that standard transformers are rarely a local optimum in the space of architectures. We show that alternative designs can perform better, but they often sacrifice universality. This calls for future work on architectures that could serve multiple objectives such as fluency and robust reasoning.

1 INTRODUCTION

Inductive biases of transformers. The recent history of machine learning has seen a uniformization of models across tasks and modalities. Most state-of-the-art models for vision, language, and speech for example are based on transformers, barring only relatively minor differences (Vaswani et al., 2017). The success of this general solution over task-specific designs has prompted the hypothesis that transformers implement very generic inductive bias¹ such as a *simplicity bias* akin to Occam’s razor (Goldblum et al., 2023). The simplicity bias of neural networks depends on architectural choices such as their activation functions (Teney et al., 2024; 2025). Yet, considering the space of all possible architectures, the following question remains (Q1).

Are transformers a unique and optimal solution endowed with generic inductive biases?

Uneven performance across domains. Transformers perform remarkably well for many applications, e.g. when trained as large language models (LLMs). Paradoxically, they also fail to learn elementary tasks such as arithmetic operations (Nikankin et al., 2024). These failures demonstrate limitations of transformers and have motivated new designs such as positional encodings (Cai et al., 2025; Jelassi et al., 2024) and alternative attention mechanisms (Katharopoulos et al., 2020; Saratchandran et al., 2024b; Schlag et al., 2021). But these new designs are rarely adopted beyond toy tasks. This suggests that the inductive biases of standard transformers are not as well suited to domains as different as e.g. natural language and arithmetic. This raises another question (Q2).

Should we even seek to address such different domains with the same learning method?

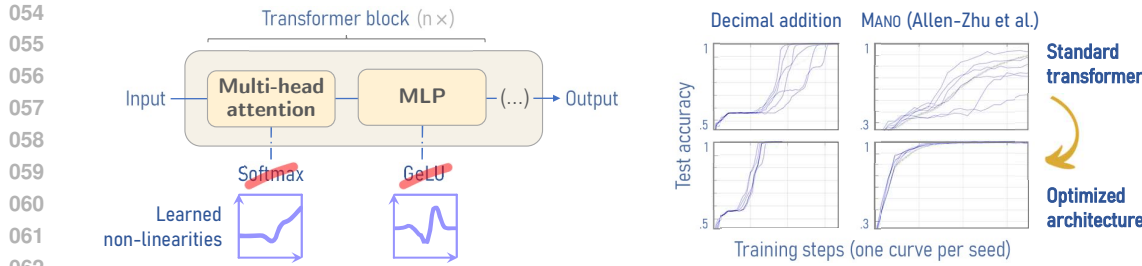


Figure 1: **Our approach to discover better task-specific inductive biases.** (Left) We replace the main non-linearities in a transformer (softmax, GeLUs) with parametrized components optimized for specific tasks. (Right) The optimized architectures allow us to train models with dramatically better convergence, generalization, and stability across seeds, on algorithmic tasks and code/language modeling datasets. We also mix-and-match the new architectures across tasks (not pictured) to evaluate the compatibility of inductive biases across tasks.

The above questions matter for developing future learning systems. Although recent progress in AI stems from scaling up models and data (Mayilvahanan et al., 2025), this growth is not infinitely sustainable, and better learning efficiency seems possible given the capabilities of biological systems. This fundamentally requires improving the inductive biases of our learning methods. Understanding the inductive biases of transformers (Q1) is a step in this direction. And understanding the compatibility of different tasks (Q2) will help select better proxies and incentives for future progress.

Our approach. We address the above questions with a method that optimizes the inductive biases for a specific task by tweaking the transformer architecture. We replace non-linearities (GeLUs, softmax) with parametrized ones, optimized on held-out data. This yields new architectures that match or surpass standard transformers. The improvement in learning speed and/or generalization indicates how far the standard transformer is from a local optimum in the space of architecture for a specific task (Q1). We also mix-and-match these new architectures across tasks to assess how the inductive biases tuned for one task perform for another, thus assessing their compatibility (Q2).

Findings. We study two domains: algorithmic skills and language modeling. For algorithmic skills, we use toy tasks commonly used to evaluate architectures, see e.g. Allen-Zhu (2025). For nearly all considered tasks, our approach finds architectures that dramatically improve learning speed, generalization, and stability across random seeds (Section 3.1). Task-specific variants of transformers can thus be **vastly superior to standard designs, using only minor modifications** like replacing the GeLUs. Our cross-task evaluation also reveals that the new architectures are quite task-specific. This can explain why many hand-crafted components from the literature (e.g. attention mechanisms, positional encodings) are rarely adopted beyond toy tasks. It also challenges the view that a single architecture can be optimal for a vast set of tasks (Goldblum et al., 2023).

For language modeling, we evaluate multiple datasets of natural language and computer code. In most cases, we also find optimized architectures that slightly improve over a baseline transformer. We stress that these improvements are practically not directly useful, because standard components are more computationally efficient. But they matter indirectly, because they are evidence that **standard transformers are neither a unique nor a local optimum** in the space of architectures. In contrast to algorithmic tasks, the cross-task evaluation shows that the improvements can transfer across natural language datasets and tokenization levels (character vs. subword). Overall, the results suggest that standard transformers are intrinsically better suited to modeling natural language than code, and clearly ill-equipped to learn algorithmic skills.

Our contributions are summarized as follows.

- **A method to optimize a transformer architecture** for any given dataset (Section 2). We replace GeLUs and softmaxes with parametrized components optimized on held-out data. The optimized architecture can then be used with standard training to evaluate its suitability to any other dataset.

¹The *inductive biases* of a learning algorithm correspond to a prior over the space of functions (Mitchell, 1980; Mingard et al., 2021) that favors particular (types of) functions among the many that fit the data. We focus on biases encoded in architectures, rather than choices of optimizer, objective function, initialization, etc.

- **An application to algorithmic tasks** (Section 3). We find that optimized architectures dramatically improve learning speed, generalization, and stability across seeds. They also prove very task-specific, showing the utility of inductive biases very different from standard transformers’.
- **An application to language modeling** (Section 4). We obtain small, albeit consistent improvements, showing that standard transformers are neither unique nor optimal designs, even for common code and natural language modeling tasks.

We discuss implications for the development of future learning systems in Section 6.

2 PROPOSED METHOD TO OPTIMIZE AND EVALUATE ARCHITECTURES

Goal. We consider, as a baseline architecture, a standard decoder-only transformer (GPT-2-style, see details in Appendix B). Our goal is to evaluate whether this choice is optimal for specific tasks and datasets. We also seek to identify better variants, as a proxy for identifying the inductive biases best suited to each task. Evaluating the new architectures across tasks can then measure the compatibility of pairs of tasks. All the tasks we consider are formulated as sequence completion of natural language, computer code, or abstract tokens.

Replacing non-linearities with parametrized functions. We replace the main non-linearities in a transformer with parametrized components that can be optimized (see Figure 1). Indeed, the main difference between a transformer and a simple linear model hinge on a few non-linear operations in the attention and MLP layers, which we will alter to obtain different inductive biases.

- An MLP layer is defined as: $\mathbf{x} \leftarrow \mathbf{W}' \phi(\mathbf{W}\mathbf{x} + \mathbf{b}) + \mathbf{b}'$ where \mathbf{x} is a vector of activations, \mathbf{W} , \mathbf{W}' , \mathbf{b} , \mathbf{b}' learned weights and biases, and $\phi: \mathbb{R} \rightarrow \mathbb{R}$ an element-wise non-linearity. In the baseline architecture, ϕ is a GeLU. In our model, $\phi_{\theta_{\text{MLP}}}$ is a 1D linear spline parametrized by learnable keypoints θ_{MLP} , capable of approximating a variety of functions (details in Appendix B).
- An attention layer in the baseline transformer is defined as: $\mathbf{x} \leftarrow \text{softmax}(\mathbf{Q}\mathbf{K}^\top)\mathbf{V}$, where \mathbf{x} is the output vector of activations and $\mathbf{Q}, \mathbf{K}, \mathbf{V}$ are linear projections of the input. This is a special case of the kernel version of attention: $\mathbf{x} \leftarrow \sum_{j=1}^n K(\mathbf{Q}_i, \mathbf{K}_j) \mathbf{V}_j / \sum_{j=1}^n K(\mathbf{Q}_i, \mathbf{K}_j)$ where the similarity between \mathbf{Q} and \mathbf{K} is measured with a kernel function $K(\mathbf{Q}, \mathbf{K})$. In the baseline transformer, $K_{\text{smax}}(\mathbf{Q}, \mathbf{K}) = \exp(\mathbf{Q}^\top \mathbf{K} / \sqrt{d})$. In our model, we introduce a learnable non-linearity $\phi': \mathbb{R} \rightarrow \mathbb{R}$ giving $K(\mathbf{Q}, \mathbf{K}) = \phi'(\mathbf{Q})^\top \phi'(\mathbf{K})$. We implement ϕ' as a linear spline ϕ'_{θ_A} with keypoints θ_A that can be optimized.

Two-stage setting. Our experiments proceed in two stages. In stage I, we optimize the architecture for a chosen dataset \mathbb{D} by training both the model’s weights and its parametrized non-linearities ($\theta_A, \theta_{\text{MLP}}$) on \mathbb{D} . In stage II, the non-linearities are frozen, and we retrain the model in a standard manner from scratch on any dataset \mathbb{D}' . The models obtained from stage II are thus fairly comparable with the baseline architecture.² When $\mathbb{D}' \neq \mathbb{D}$, i.e. a “mix-and-match” setting, stage II serves to evaluate whether the inductive biases optimized for \mathbb{D} suit the learning of \mathbb{D}' .

Optimizing architectures. Our method may seem similar to prior work about learning activation functions (e.g. (Alexandridis et al., 2025)) but their goals are very different. These works seek to improve performance by continuously updating the activation during training. Whereas we seek to identify inductive biases that can remain hard-encoded in the architecture and further reused to train new models with other seeds and datasets (stage II). We make this possible with a **two-loss training**. During stage I, we hold out a fraction of the training data (e.g. 20%) that we use solely for optimizing the non-linearities, while we optimize the weights in a standard manner on the training set. This prevents a co-adaptation, that could make the non-linearities overfit particular weights or seed. This is particularly important for our experiments on algorithmic toy tasks, and even more so for improving length generalization³ (Section 3.1). In this latter case, we hold out an out-of-distribution (OOD) split of data (see Section 3.1), such that the weights are optimized for one range of sequence lengths, and the architecture for a different wider range. This forces the architecture to capture an inductive bias for length generalization. In stage II, the non-linearities are frozen, and the model weights are trained in a standard manner on the whole training split of the target dataset.

²In stage II, $(\theta_A, \theta_{\text{MLP}})$ are frozen and better viewed as pre-tuned hyperparameters than extra model capacity.

³The benefit of the two-loss training is smaller for language modeling because the models are heavily over-parametrized and never at risk of overfitting the training data.

162 A second innovation to prevent the co-adaptation of weights and non-linearities in stage I is **multi-**
 163 **model training**. We train M models in parallel (e.g. $M = 4$) that use different seeds but share
 164 the non-linearities being optimized. The resulting optimized architecture is naturally more likely to
 165 generalize in stage II to other weights and datasets (see Appendix D). This also proves particularly
 166 helpful for algorithmic tasks because the variance across seeds of the baseline architecture is often
 167 high. We provide a complete description of our method as Algorithm 1 in the appendix.

168 **Rational for splines.** We parametrize our non-linearities as linear splines because they offer the
 169 most unbiased tractable parametrization for an $\mathbb{R} \rightarrow \mathbb{R}$ function. For example, a spline can represent
 170 the identity function as easily as a step function or a sine wave. Prior work on trainable activation
 171 functions enforces priors of smoothness or monotonicity e.g. with small MLPs (Apicella et al., 2021;
 172 Greydanus & Kobak, 2020)). These would struggle to capture sharp transitions like in Figure 6. We
 173 also favor *linear* splines over higher-order (e.g. cubic) ones because they behave nearly identically
 174 while being much cheaper, as evaluated by Teney et al. (2025, Appendix D).

3 EXPERIMENTS ON ALGORITHMIC REASONING TASKS

178 In this section, we apply the proposed method to a set of tasks commonly used to evaluate the
 179 algorithmic skills of transformers, detailed in Table 1. These tasks are elementary but remarkably
 180 challenging and often used to highlight limitations of transformers. All the tasks are formulated as
 181 sequence completion. Each sequence comprises an “input” part, followed by a separator then an
 182 “output” part. The models are trained with a next-token prediction objective on the latter part of
 183 training sequences. Unless otherwise noted we use i.i.d. sets of training, validation, and test data.

184 **Experimental setup.** For each task \mathbb{D} , we first train the baseline architecture and tune its hyper-
 185 parameters (width, depth, learning rate, batch size, etc.) for high accuracy and fast convergence on
 186 the validation set. We then run the proposed method (stage I, $M = 8$) to optimize the architecture
 187 for \mathbb{D} . We then re-train a model from scratch with the optimized architecture (stage II), keeping the
 188 same hyperparameters (we saw no further improvements by re-tuning them). In Section 3.2, we also
 189 re-train models on other tasks \mathbb{D}' as a way to evaluate the generality of the optimized architecture
 190 and the compatibility of \mathbb{D} and \mathbb{D}' . All results are averages over 6 random seeds.

191 Table 1: Algorithmic tasks used in our experiments. They are similarly-sized in term of complexity
 192 and required model capacity, except for MANO (Allen-Zhu, 2025) which is relatively more complex.

Task	Examples
MEMORIZIZE. Simple memorization of a mapping between a two-integer key and an integer value, with all integers in $[1,32]$. Each sequence consists of the key, a separator, and the value. This task has no test set: performance is simply the training accuracy (Zhong & Andreas, 2024).	23 12 10 11 32 27 31 19 18
PARENTHESES. Recognition of Dyck language. Each sequence contains parentheses followed by a separator and a marker indicating whether they are balanced or not. Sequences lengths are in $[1,20]$ in the training set, and $[21,40]$ in the validation and test sets (Zhong & Andreas, 2024).	() (<unbalanced> (() ()) <balanced>) () <unbalanced>
ADDMOD. Modular addition mod N , with 95% of the N^2 examples used for training (Zhong & Andreas, 2024). We use $N=97$.	12 3 15 96 2 1
HAYSTACK. Needle-in-a-haystack recall. The model gets a sequence $[m_1, c_1 \dots m_k, c_k, m_u]$ of markers m_u and values c_k . It must search for the first occurrence of m_u and return its successor c_u (Zhong & Andreas, 2024). We use $k \in [1,10]$ and $m_k, c_k \in [1,64]$.	2 p 9 k 3 b 9 k 8 a 2 b 8 a 2 p 9 k 3 b 5 x 5 x
ADD. Decimal addition of 4-digit numbers with digit-wise tokens. (Zhong & Andreas, 2024).	1 0 0 9 + 1 0 9 2 2 1 0 1
ADDREVERSED. ADD with reversed numbers, known to be easier to learn (Lee et al., 2023).	9 0 0 1 + 2 9 0 1 1 0 1 2
COPY. Repeating the input. Elementary but unsolved for length generalization (Cai et al., 2025). Tokens in $[1,8]$. Seq. lengths in $[2,10]$ for training, $[2,15]$ for validation, $[16,20]$ for testing.	2 8 2 8 9 4 8 7 8 3 9 4 8 7 8 3
MANO. Synthetic task proposed by Allen-Zhu (2025) to evaluate large pretrained models. Each sequence specifies nested arithmetic operations mod N with number-level tokens. Our scaled-down version uses $N=7$ and a number of operations per sequences in $[1,3]$.	(1*3)+4 0 (2-(6-1))*3 5 (3*(5-6))-1 3

3.1 IMPROVEMENTS ON INDIVIDUAL TASKS

212 **Faster convergence.** The most striking improvement with optimized architectures is the learning
 213 speed (Figure 2). For the ADD and MANO tasks for example, convergence occurs $2\text{--}3\times$ faster. The
 214 learning rate of the baseline was tuned to its maximum stable value for every task.

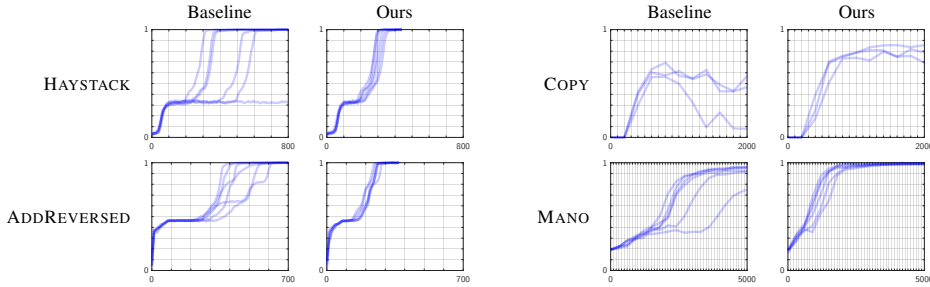


Figure 2: Training curves (test accuracy vs. training step, one curve per random seed) of models trained on algorithmic tasks with a baseline transformer or our optimized architectures. The latter converge much faster and show less variance across seeds. See Appendix C for other tasks.

Reduced variance. On some tasks, baseline transformers show huge variance in accuracy and training speed across random seeds. This suggests tasks that are underspecified (Teney et al., 2021; 2022) and misaligned with the model’s inductive biases (Zhou et al., 2024). In these cases, the optimized architectures eliminate the problem and make the training much more reliable (Figure 2).

Better generalization. For some tasks, baseline transformers do not reach perfect test accuracy though they perfectly fit the training data. This shows again a misalignment between the target function and the inductive biases. Optimized architectures solve this problem (see e.g. MANO, Figure 2).

Improved length generalization. An outstanding challenge for transformers is the generalization to sequences longer than seen during training. Even the COPY task is unsolved and a baseline transformer completely fails on unseen lengths (Figure 3). Among the plethora of existing partial solutions, the Alibi positional encodings (Press et al., 2021) bring non-trivial accuracy on slightly longer sequences. We use our method to optimize the Alibi architecture. We use the two-loss mechanism of Algorithm 1 to optimize the transformer weights on lengths 2–10 and the non-linearities on 2–15. This forces the optimized architecture to capture an inductive bias for length generalization. As a result, a model trained with the optimized architecture reaches higher accuracies on longer sequences. While this is not a complete solution to length generalization, it shows that inappropriate inductive biases in the base architecture are one of the obstacles to length generalization.

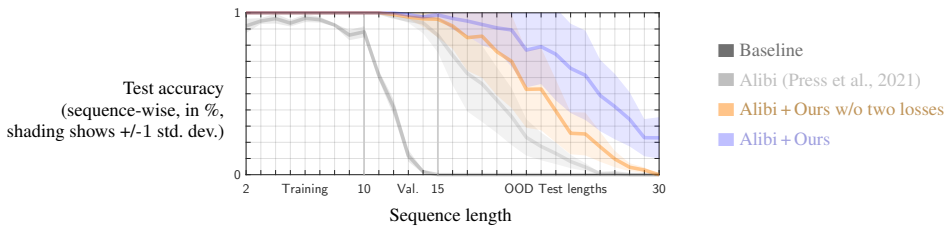


Figure 3: Length generalization on the COPY task. The baseline completely fails on unseen lengths ($\gg 10$). Alibi positional encodings (Press et al., 2021) help. Optimizing the Alibi architecture with our method further improves the accuracy and extends the benefits to longer sequences.

Performance with smaller models. We train models of different widths for each task. Results in Figure 4 show that the accuracy drops more sharply on some tasks with the baseline architecture than optimized ones. Intuitively, when the architecture is already aligned with the task, less capacity is needed in its weights. Equivalently, a fixed number of parameters offers more capacity.

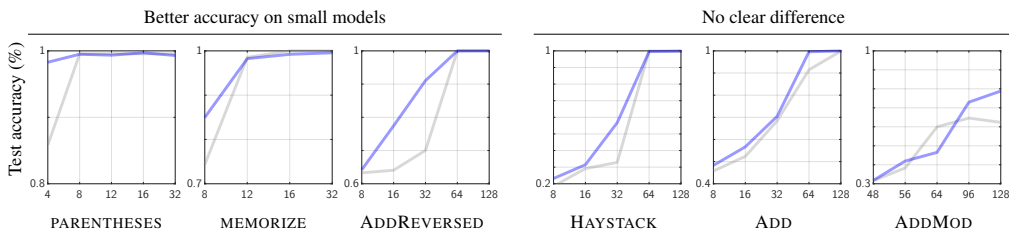


Figure 4: Test accuracy of models of different widths (X axis). On some tasks, optimized architectures (blue) maintain higher accuracy than the baseline (grey) when reducing the width of the model.

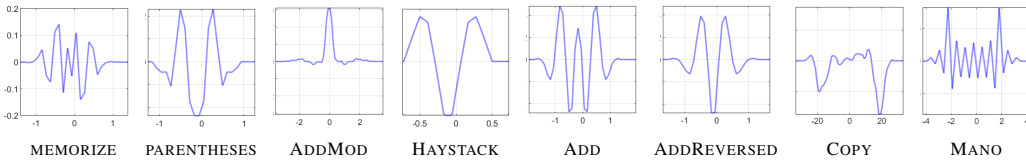
270 3.2 COMPATIBILITY OF OPTIMIZED ARCHITECTURES ACROSS ALGORITHMIC TASKS
271

272 We now train models on each task \mathbb{D} using architectures optimized for any other task \mathbb{D}' to evaluate
273 the pairwise compatibility of their inductive biases. The results in Figure 5 show that the optimized
274 architectures are very task-specific. Few of the benefits transfer across tasks, mostly across closely
275 related tasks like ADD and ADDREVERSED. Many perform worse than a standard transformer. This
276 shows that the specialization to our algorithmic tasks comes at the cost of universality. These tasks
277 are very narrow however and it remains an open question whether the negative impact is inevitable.
278 A future step to study this question could be a multi-task optimization in Algorithm 1.

	Memorize	AddMod	Add	AddReversed	Mano	Haystack	Copy	Parentheses	
Architectures optimized for specific tasks	Memorize	+43	+0	+9	+13	-4	-10	-15	+0
	AddMod	+16	+16	+14	+21	-1	-9	+6	-4
	Add	+17	+7	+15	+18	+29	+7	+13	+0
	AddReversed	+14	+6	+14	+17	+29	+6	+12	+1
	Mano	+9	+3	+9	+12	+22	+13	+17	+0
	Haystack	+1	+3	+8	-2	-6	+12	+15	-0
	Copy	-0	+3	+11	-3	-11	+11	+19	-1
	Parentheses	+7	+5	+9	+10	+13	+11	+13	+0

291 Target tasks

292 Figure 5: Compatibility of architectures across algorithmic tasks. We plot the absolute difference in
293 test accuracy (%) with the baseline after a fixed number of steps (details in Appendix B). The best
294 option per task (column) is usually on the diagonal, meaning that the optimized architectures are
295 quite task-specific, while still yielding some positive transfer.



302 Figure 6: MLP non-linearities optimized for each algorithmic task.
303

304 **Take-away.** On algorithmic tasks, optimized architectures can dramatically outperform standard
305 transformers, but the benefits are quite task-specific. This means that these tasks require inductive
306 biases very different from those of standard transformers.
307

308 4 EXPERIMENTS ON LANGUAGE MODELING TASKS
309

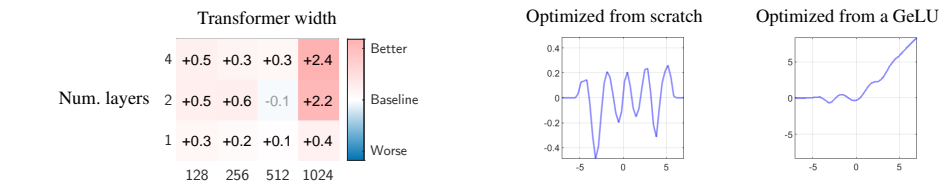
310 We now apply the same experimental setup as Section 3 to language modeling. We use datasets
311 for computer code (English, Java) and natural language of various complexity levels (Table 2). Our
312 goal is to understand whether different type of data benefit from different inductive biases. Current
313 practices for building LLMs show that data diversity is beneficial (Longpre et al., 2024) and that
314 code is complementary to natural language (Aryabumi et al., 2024; Petty et al., 2024). But because
315 all kinds of data are mixed during training, it is unknown whether they could each exploit or elicit
316 different mechanisms in a model. We also consider versions of the datasets tokenized at the character
317 or subword level (BPE; details in Appendix B). These choices are motivated by Mayilvahanan et al.
318 (2025) who showed that LLM performance is mostly determined by data diversity and tokenization.
319

320 4.1 IMPROVEMENTS ON INDIVIDUAL DATASETS
321

322 **TINYSTORIES.** We compare in Figure 7 models trained with baseline or optimized architectures.
323 The latter do slightly better. The improvement is small but consistent at different model sizes. Training
324 curves (Figure 15) show that the improvement is larger early during training then diminishes. We

324 Table 2: Datasets used in our experiments for language modeling (see Appendix B for details).
325

326 Dataset	327 Excerpt
327 TINYSTORIES. Children stories generated with GPT-3.5. It was designed to capture core aspects 328 of natural language (syntax, coherence, compositionality) with a limited vocabulary. This allows 329 smaller-scale experiments than web-scale open-domain corpora (Eldan & Li, 2023).	328 Once upon a time, there was 329 a clever little dog named 330 Max. Max loved to run (...)
330 SHAKESPEARE. Plays and sonnets by William Shakespeare, often used in early research on 331 language modeling. It includes recognizable patterns of grammar, rhythm, and vocabulary, as 332 well as a unique structure because of the speaker labels and dialogue formatting (Karpathy, 2015).	331 BENVOLIO: Good-morrow, 332 cousin. ROMEO: Is the day 333 so young? BENVOLIO: But (...)
332 ENWIK8. First 100 M bytes of the English Wikipedia (Mahoney, 2006). We use the clean version 333 from Yong (2025) with only text visible to human readers, without links and meta data. This data 334 provides dense, real-world text with a mix of vocabulary, syntax, and formatting.	334 anarchism originated as a 335 term of abuse first used 336 against early working (...)
337 CODESEARCHNET-JAVA & -PYTHON. Dataset of computer code originally created to support 338 research on code search and code-text understanding (Husel et al., 2019). We discard comments 339 and descriptions in natural language following Lu et al. (2021) to focus exclusively on code.	339 batch, limit = 100, 340 self.next_limit() 341 it = iter(it) (...)

343 Figure 7: **(Left)** Absolute improvements in token prediction accuracy (%) of the best optimized
344 architectures on TINYSTORIES compared to our baseline transformer. The accuracy is consistently
345 slightly better at different model sizes. **(Right)** Visualization of MLP non-linearities optimized from
346 scratch (results on the left) or from a GeLU initialization (*GeLU + Ours* in Figure 8). Although they
347 resemble generic wavelets, we show in Appendix D that fine details in these functions matter.
348349 find it best to optimize non-linearities only in MLPs (i.e. replacing GeLUs; see Figure 8). Replacing
350 softwares with learned components barely matches or underperforms the baseline, indicating a
351 difficult optimization. We experimented with alternative parametrizations that exactly mimic a soft-
352 max at initialization. This solution would barely move away from this initialization (not reported in
353 tables), suggesting that a softmax is close to a local optimum.354 We visualize in Figure 7 (right) the optimized MLP non-linearities, which are remarkably similar to
355 sine wavelets. We evaluate a non-exhaustive selection of activation functions and attention variants
356 from the literature in Table 3. None of them works better than ours. The gated linear units (GLUs)
357 are a popular design that adds multiplicative interactions to the MLPs. We show that we can also
358 improve them by introducing our learned spline in GLUs in lieu of their internal Swish activations.
359 This provides similar improvements as over standard MLPs, cf. *GLU/Swish* and *GLU/Ours* in Table 3.
360 We also evaluate in Appendix D the importance of fine details in the learned non-linearities. We try
361 to make them more periodic or symmetric, but they then always perform worse.
362362 Table 3: Performance of models trained on TINYSTORIES with existing alternative attention and
363 MLP designs (2 layers, width 256). None works better than ours. See Appendix D for references.
364

365 Attention	366 MLP	smax	smax	smax	smax	smax	smax	smax	smax	P1	P3	Adaptive	NormSmax
365 MLP	366	Linear	GeLU	Ours	GLU/Swish	GLU/Ours	ReLU	ReLU ²	TanH	Sinc	Gaussian	GeLU	GeLU
367 Tr. perplexity	1.78	1.58	1.57	1.59	1.58	1.60	1.60	1.71	2.50	1.64	1.62	1.60	1.58
367 Val. acc. (%)	59.9	63.7	64.4	63.7	64.0	63.5	63.6	61.2	47.7	62.8	63.0	63.7	63.7

369 **SHAKESPEARE & ENWIK8.** These datasets differ from TinyStories in their richer vocabulary and
370 sentence structure. SHAKESPEARE also follows a particular formatting presenting dialogues with
371 speaker labels (see Table 2). The results in Figures 8 & 13 show that *some* optimized architectures
372 slightly improve over the baseline. Optimizing non-linearities in the MLPs is again more useful
373 than in the attention. However, differences with the baseline are small, which suggests that standard
374 transformers are inherently well suited to language modeling.
375376 The improvement is slightly clearer on **character-level datasets** than on tokenized ones (marked
377 -CHAR in Figure 8). We hypothesize that the target function to be learned by the transformer layers
378 for character-level language modeling is more complex, because of the lesser capacity available

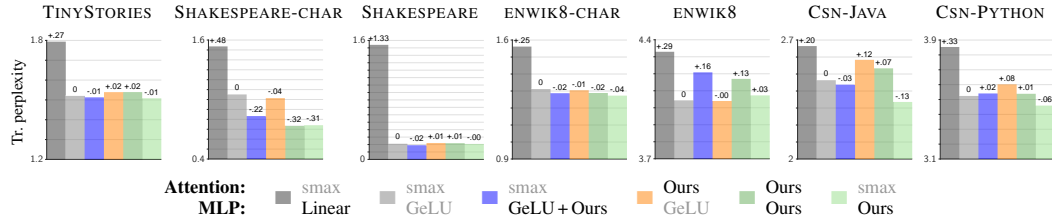


Figure 8: Perplexity on code and natural language (lower is better; numbers on bars correspond to the difference with the baseline architecture). Some optimized architectures perform slightly better than the baseline, often simply with optimized MLP non-linearities (green). Datasets of code (CSN-JAVA, CSN-PYTHON) also benefit relatively more than datasets of natural language.

in the model’s token embeddings (embeddings can otherwise make up a significant fraction of the model parameters for tokenized datasets). This could be the reason why learned non-linearities are particularly helpful, since they can help learn and represent complex functions (Teney et al., 2025).

We also evaluate a version of our optimized **MLP non-linearities initialized as a GeLU** rather than a constant zero (*GeLU + Ours* in Figure 8). With this, the model starts stage I with a non-linearity known to perform well. And because the optimization is non-convex, the optimized solution remains in the local search space near GeLUs (see Figure 7, right). The models trained with these non-linearities perform in-between GeLUs and those optimized from scratch. This means that GeLUs are usually not an optimal solution, not even a local one. But note also that our best solutions are not guaranteed to be *globally* optimal and better ones may exist.

CODESEARCHNET (CSN-JAVA, CSN-PYTHON). The results in Figure 8 show that our optimized non-linearities in MLPs improve again over the baseline. The gains are larger for code than natural language, relative to the gap between the baselines with linear and GeLU MLPs. These larger gains may reflect the larger importance of systematic structure and compositionality in code than natural language. The task of modeling code may thus resemble some of the algorithmic tasks of Section 3, which benefited greatly from optimized architectures. Therefore, the architectures best suited to natural language may not be simultaneously optimal for code.

4.2 COMPATIBILITY OF OPTIMIZED ARCHITECTURES ACROSS LANGUAGE DATASETS

Our final results examine the compatibility of the optimized architectures across language modeling datasets. We consider our seven datasets plus MANO, the most complex of our algorithmic tasks. We train models for every task \mathbb{D} using architectures optimized for any other task \mathbb{D}' . The results in Figure 9 show that the variations across architectures are very small. This contrasts with the results on algorithmic tasks (Figure 5). These optimized architectures thus encode much less task-specific specialization. This suggests that the skills required across code and language modeling datasets are much more uniform. We discuss the implications of these results in Section 6.

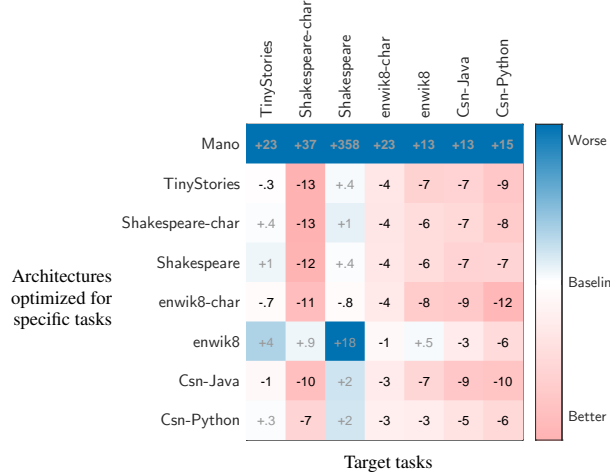


Figure 9: Compatibility of architectures across code and language datasets (relative difference in perplexity with the baseline in %, lower is better). The differences are much less dramatic than with algorithmic tasks (Figure 5), indicating smaller benefit in dataset-specific specialization.

432
433
434
435
436

Take-away. For code and natural language modeling, the optimized architectures improve much less than for algorithmic tasks. This means that standard transformers are intrinsically closer to a local optimum in the space of architecture for these tasks than for learning algorithmic skills.

437
438

5 RELATED WORK

439

Understanding inductive biases in NNs. Much of the prior on understanding neural networks (NNs) has focused on their simplicity bias, i.e. their preference for representing functions of low Kolmogorov (Zhou et al., 2023) or spectral complexity (Bhattamishra et al., 2022). The simplicity bias depends primarily on the choice of activation function (Mingard et al., 2019; Teney et al., 2024), and its suitability was questioned (Domingos, 1999) by evaluating alternative activation functions in MLPs (Teney et al., 2024). We extend this inquiry to transformers and larger settings. In particular, we introduce a method to optimize non-linearities in both attention and MLP layers, and apply it to tasks relevant to the state of the art (code, natural language, algorithmic reasoning).

447

Improving transformers. Current LLMs all use very similar architectures, and Mayilvahanan et al. (2025) show that small design differences play little role in their performance. Prior work has however studied at length the impact of various components of transformers including their nonlinearities (Jha & Reagen, 2025; Newhouse et al., 2025). Proposed improvements include alternative attention mechanisms (Katharopoulos et al., 2020; Saratchandran et al., 2024b; Schlag et al., 2021; Tamayo-Rousseau et al., 2025; Veličković et al., 2024) and activation functions for MLPs (Hu et al., 2025; Teney et al., 2025) and transformers (Mirzadeh et al., 2023; So et al., 2021a). This motivates our work by suggesting that standard transformers are not a uniquely optimal choice of architecture.

455

Architecture search. Our method to optimize architectures is reminiscent of neural architecture search (NAS) (Goyal et al., 2019; Hong, 2025; Liu et al., 2018; Manessi & Rozza, 2018; Ramachandran et al., 2018; Zoph & Le, 2017). The goals and approach are different though. NAS uses RL or evolutionary algorithms to search through pre-defined design choices. We directly use gradient descent to optimize a relatively unrestricted parametrization of the non-linearities of transformers. Our goal is not to find better models (our designs are often computationally expensive). Instead, our method is a tool to understand the compatibility of the inductive biases required for various tasks.

462

6 DISCUSSION

464

We have presented a method to optimize a transformer architecture for specific datasets and used it to study the compatibility of inductive biases across tasks. We found that standard transformers are often suboptimal, but minor tweaks (replacing GeLUs and softmax operations) can substantially improve training speed, generalization, capacity, and stability across random seeds.

469

Our results show that different tasks benefit from different inductive biases, aligning with the no-free-lunch theorem (Wolpert, 1996). Yet, transformers seem uniquely suitable to a vast range of applications (Goldblum et al., 2023): our results can be seen as probing the limits of this hypothesis.

472

Architecture vs. scale. Prior work showed that the choice of architecture can become less important with scale (Bachmann et al., 2023; Tay et al., 2022). But this also means that the current need to build ever-larger models may be due to suboptimal inductive biases. In this work, we tweaked transformers to explore the space of inductive biases, but similar effects may be achievable with other means e.g. completely different architectures, initializations (Shinnick et al., 2025), or optimizers.

477

Do we need domain-specific models? Our results show a higher compatibility across language/code than algorithmic tasks, which are often used to highlight limitations e.g. for length generalization. If these toy tasks really represent desirable capabilities in LLMs, perhaps new architectures are required to combine language and algorithmic capabilities. A future step could be to apply our method to optimize architectures for multiple tasks simultaneously.

482

Other domains. An extension of this work could examine possible improvements to transformers for other domains such as vision and speech, and whether the improvements transfer across domains.

485

486 **Limitations.** First, our **search space of architectures** is limited. Complex forms of attention
 487 (Hashemi et al., 2025) or interactions like gated linear units (GLU, Shazeer (2020)) cannot be rep-
 488 resented in our formulation. Further gains are possible with a larger search space, the optimization
 489 also becomes more challenging. Second, the **scale of our experiments** is tiny relative to state-
 490 of-the-art LLMs. The effects of different architectures may vanish with more data, but improving
 491 data efficiency is a key objective of this line of work. So the effects at small scale are particularly
 492 relevant. Third, our architectures with optimized non-linearities are **computationally costly**. Our
 493 claims are not centered on the performance of these architecture though. They serve instead to better
 494 understand the landscape of possible designs for future AI models.

495 **REPRODUCIBILITY STATEMENT**

496 Appendix B provides a formal description of the proposed method with the values of all hyperpa-
 497 rameters. Code is available at <http://github.com/anonymized/anonymized>.

500 **REFERENCES**

502 Konstantinos Panagiotis Alexandridis, Jiankang Deng, Anh Nguyen, and Shan Luo. Adaptive para-
 503 metric activation. In *ECCV*, 2025.

505 Zeyuan Allen-Zhu. Physics of Language Models: Part 4.1, Architecture Design and the Magic of
 506 Canon Layers. *SSRN Electronic Journal*, May 2025.

507 Cem Anil, Yuhuai Wu, Anders Andreassen, Aitor Lewkowycz, Vedant Misra, Vinay Ramasesh, Am-
 508 brose Slone, Guy Gur-Ari, Ethan Dyer, and Behnam Neyshabur. Exploring length generalization
 509 in large language models. *NeurIPS*, 2022.

511 Andrea Apicella, Francesco Isgro, and Roberto Prevete. A simple and efficient architecture for
 512 trainable activation functions. *Neurocomputing*, 2019.

513 Andrea Apicella, Francesco Donnarumma, Francesco Isgrò, and Roberto Prevete. A survey on
 514 modern trainable activation functions. *Neural Networks*, 2021.

516 Sanjeev Arora, Nadav Cohen, Wei Hu, and Yuping Luo. Implicit regularization in deep matrix
 517 factorization. *NeurIPS*, 2019.

518 Viraat Aryabumi, Yixuan Su, Raymond Ma, Adrien Morisot, Ivan Zhang, Acyr Locatelli, Marzieh
 519 Fadaee, Ahmet Üstün, and Sara Hooker. To code, or not to code? exploring impact of code in
 520 pre-training. *arXiv:2408.10914*, 2024.

522 Gregor Bachmann, Sotiris Anagnostidis, and Thomas Hofmann. Scaling MLPs: A tale of inductive
 523 bias. *arXiv:2306.13575*, 2023.

524 Samuel James Bell and Levent Sagun. Simplicity bias leads to amplified performance disparities.
 525 In *Proceedings of the 2023 ACM Conference on Fairness, Accountability, and Transparency*, pp.
 526 355–369, 2023.

528 Satwik Bhattacharya, Arkil Patel, Varun Kanade, and Phil Blunsom. Simplicity bias in transformers
 529 and their ability to learn sparse boolean functions. *arXiv:2211.12316*, 2022.

531 Garrett Bingham, William Macke, and Risto Miikkulainen. Evolutionary optimization of deep learn-
 532 ing activation functions. In *Genetic and Evolutionary Computation Conference*, 2020.

533 Ziyang Cai, Nayoung Lee, Avi Schwarzschild, Samet Oymak, and Dimitris Papailiopoulos. Ex-
 534 trapolation by association: Length generalization transfer in transformers. *arXiv:2506.09251*,
 535 2025.

536 Irit Chelly, Shahaf E Finder, Shira Ifergane, and Oren Freifeld. Trainable highly-expressive activa-
 537 tion functions. In *ECCV*. Springer, 2024.

539 CodeGPT. Microsoft CodeGPT (available on HuggingFace), 2024. <https://huggingface.co/microsoft/CodeGPT-small-py>.

540 Giacomo De Palma, Bobak Kiani, and Seth Lloyd. Random deep neural networks are biased towards
 541 simple functions. *NeurIPS*, 2019.

542

543 Kamaludin Dingle, Chico Q Camargo, and Ard A Louis. Input–output maps are strongly biased
 544 towards simple outputs. *Nature communications*, 2018.

545 Pedro Domingos. The role of occam’s razor in knowledge discovery. *Data mining and knowledge
 546 discovery*, 1999.

547

548 Shiv Ram Dubey, Satish Kumar Singh, and Bidyut Baran Chaudhuri. Activation functions in deep
 549 learning: A comprehensive survey and benchmark. *Neurocomputing*, 2022.

550 Stanislas Ducotterd, Alexis Goujon, Pakshal Bohra, Dimitris Perdios, Sebastian Neumayer, and
 551 Michael Unser. Improving lipschitz-constrained neural networks by learning activation functions.
 552 *Journal of Machine Learning Research*, 2024.

553

554 Nouha Dziri, Ximing Lu, Melanie Sclar, Xiang Lorraine Li, Liwei Jiang, Bill Yuchen Lin, Sean
 555 Welleck, Peter West, Chandra Bhagavatula, Ronan Le Bras, et al. Faith and fate: Limits of
 556 transformers on compositionality. *NeurIPS*, 36, 2023.

557 Ronen Eldan and Yuanzhi Li. Tinystories: How small can language models be and still speak
 558 coherent english? *arXiv:2305.07759*, 2023.

559

560 Richard Futrell and Kyle Mahowald. How linguistics learned to stop worrying and love the language
 561 models. *Annual Review of Linguistics*, 2023.

562 Philip Gage. A new algorithm for data compression. *C Users Journal*, 12(2):23–38, 1994.

563

564 Gallant. There exists a neural network that does not make avoidable mistakes. In *IEEE International
 565 Conference on Neural Networks*. IEEE, 1988.

566

567 Robert Geirhos, Jörn-Henrik Jacobsen, Claudio Michaelis, Richard Zemel, Wieland Brendel,
 568 Matthias Bethge, and Felix A Wichmann. Shortcut learning in deep neural networks. *Nature
 569 Machine Intelligence*, 2020.

570 Micah Goldblum, Marc Finzi, Keefer Rowan, and Andrew Gordon Wilson. The no free
 571 lunch theorem, kolmogorov complexity, and the role of inductive biases in machine learning.
 572 *arXiv:2304.05366*, 2023.

573

574 Anirudh Goyal and Yoshua Bengio. Inductive biases for deep learning of higher-level cognition.
 575 *Proceedings of the Royal Society A*, 2022.

576

577 Mohit Goyal, Rajan Goyal, and Brejesh Lall. Learning activation functions: A new paradigm of
 578 understanding neural networks. *arXiv:1906.09529*, 2019.

579

580 Sam Greydanus and Dmitry Kobak. Scaling down deep learning with MNIST-1D. *arXiv preprint
 581 arXiv:2011.14439*, 2020.

582

583 Michael Hahn and Mark Rofin. Why are sensitive functions hard for transformers?
 584 *arXiv:2402.09963*, 2024.

585

586 Michael Hahn, Dan Jurafsky, and Richard Futrell. Sensitivity as a complexity measure for sequence
 587 classification tasks. *Transactions of the ACL*, 2021.

588

589 Baran Hashemi, Kurt Pasque, Chris Teska, and Ruriko Yoshida. Tropical attention: Neural algorithmic
 590 reasoning for combinatorial algorithms. *arXiv:2505.17190*, 2025.

591

592 Dan Hendrycks and Kevin Gimpel. Gaussian error linear units (GeLUs). *arXiv:1606.08415*, 2016.

593

594 Katherine L Hermann and Andrew K Lampinen. What shapes feature representations? exploring
 595 datasets, architectures, and training. *arXiv:2006.12433*, 2020.

596

597 Jinwook Hong. Asnn: Learning to suggest neural architectures from performance distributions.
 598 *arXiv:2507.20164*, 2025.

594 Sara Hooker. The hardware lottery. *CACM*, 64(12):58–65, 2021.
 595

596 Leyang Hu, Matteo Gamba, and Randall Balestrier. Curvature tuning: Provable training-free model
 597 steering from a single parameter. *arXiv:2502.07783*, 2025.

598 Hamel Husel, Ho-Hsiang Wu, Tiferet Gazit, Miltiadis Allamanis, and Marc Brockschmidt. Code-
 599 searchnet challenge: Evaluating the state of semantic code search. *arXiv:1909.09436*, 2019.
 600

601 Ameya D Jagtap and George Em Karniadakis. How important are activation functions in regression
 602 and classification? a survey, performance comparison, and future directions. *Journal of Machine
 603 Learning for Modeling and Computing*, 4(1), 2023.

604 Ameya D Jagtap, Kenji Kawaguchi, and George Em Karniadakis. Adaptive activation functions
 605 accelerate convergence in deep and physics-informed neural networks. *Journal of Computational
 606 Physics*, 2020.

607 Samy Jelassi, David Brandfonbrener, Sham M Kakade, and Eran Malach. Repeat after me: Trans-
 608 formers are better than state space models at copying. *arXiv:2402.01032*, 2024.

609 Nandan Kumar Jha and Brandon Reagen. Entropy-guided attention for private llms.
 610 *arXiv:2501.03489*, 2025.

611 Zixuan Jiang, Jiaqi Gu, and David Z Pan. Normsoftmax: Normalizing the input of softmax to
 612 accelerate and stabilize training. In *IEEE International Conference on Omni-layer Intelligent
 613 Systems (COINS)*. IEEE, 2023.

614 Keller Jordan, Jeremy Bernstein, Brendan Rappazzo, @fernbear.bsky.social, Boza Vlado,
 615 You Jiacheng, Franz Cesista, Braden Koszarsky, and @Grad62304977. modded-nanopt:
 616 Speedrunning the nanopt baseline, 2024. URL <https://github.com/KellerJordan/modded-nanopt>.

617 Dimitris Kalimeris, Gal Kaplun, Preetum Nakkiran, Benjamin Edelman, Tristan Yang, Boaz Barak,
 618 and Haofeng Zhang. SGD on neural networks learns functions of increasing complexity. *NeurIPS*,
 619 2019.

620 Andrey Karpathy. The unreasonable effectiveness of recurrent neural networks. [http://
 621 karpathy.github.io/2015/05/21/rnn-effectiveness/](http://karpathy.github.io/2015/05/21/rnn-effectiveness/), 2015.

622 Angelos Katharopoulos, Apoorv Vyas, Nikolaos Pappas, and François Fleuret. Transformers are
 623 rnns: Fast autoregressive transformers with linear attention. In *ICML*. PMLR, 2020.

624 Amirkhossein Kazemnejad, Inkit Padhi, Karthikeyan Natesan Ramamurthy, Payel Das, and Siva
 625 Reddy. The impact of positional encoding on length generalization in transformers. *NeurIPS*,
 626 2023.

627 Jan Kukačka, Vladimir Golkov, and Daniel Cremers. Regularization for deep learning: A taxonomy.
 628 *arXiv:1710.10686*, 2017.

629 Nayoung Lee, Kartik Sreenivasan, Jason D Lee, Kangwook Lee, and Dimitris Papailiopoulos.
 630 Teaching arithmetic to small transformers. *arXiv:2307.03381*, 2023.

631 Chenxi Liu, Barret Zoph, Maxim Neumann, Jonathon Shlens, Wei Hua, Li-Jia Li, Li Fei-Fei, Alan L.
 632 Yuille, Jonathan Huang, and Kevin Murphy. Progressive neural architecture search. In *15th
 633 European Conference on Computer Vision (ECCV)*, 2018.

634 Ziming Liu, Yixuan Wang, Sachin Vaidya, Fabian Ruehle, James Halverson, Marin Soljačić,
 635 Thomas Y Hou, and Max Tegmark. Kan: Kolmogorov-arnold networks. *arXiv:2404.19756*,
 636 2024.

637 Shayne Longpre, Gregory Yauney, Emily Reif, Katherine Lee, Adam Roberts, Barret Zoph, Denny
 638 Zhou, Jason Wei, Kevin Robinson, David Mimno, et al. A pretrainer’s guide to training data:
 639 Measuring the effects of data age, domain coverage, quality, & toxicity. In *Proceedings of the
 640 Conference of the North American Chapter of the Association for Computational Linguistics*,
 641 2024.

648 Shuai Lu, Daya Guo, Shuo Ren, Junjie Huang, Alexey Svyatkovskiy, Ambrosio Blanco, Colin
 649 Clement, Dawn Drain, Dixin Jiang, Duyu Tang, et al. CodeXGlue: A machine learning bench-
 650 mark dataset for code understanding and generation. *arXiv:2102.04664*, 2021.

651 Kaifeng Lyu, Zhiyuan Li, Runzhe Wang, and Sanjeev Arora. Gradient descent on two-layer nets:
 652 Margin maximization and simplicity bias. *NeurIPS*, 2021.

653 Andrew L Maas, Awni Y Hannun, Andrew Y Ng, et al. Rectifier nonlinearities improve neural
 654 network acoustic models. In *ICML*, 2013.

655 Matt Mahoney. enwik8: First 100m bytes of english wikipedia. Available at <https://mattmahoney.net/dc/textdata.html>, 2006.

656 Franco Manessi and Alessandro Rozza. Learning combinations of activation functions. In *Inter-
 657 national Conference on Pattern Recognition (ICPR)*, 2018.

658 Prasanna Mayilvahanan, Thaddäus Wiedemer, Sayak Mallick, Matthias Bethge, and Wieland Bren-
 659 del. Llms on the line: Data determines loss-to-loss scaling laws. *arXiv:2502.12120*, 2025.

660 Raphaël Millière. Language models as models of language. *Mind & Language*, 2024.

661 Chris Mingard, Joar Skalse, Guillermo Valle-Pérez, David Martínez-Rubio, Vladimir Mikulik, and
 662 Ard A Louis. Neural networks are a priori biased towards boolean functions with low entropy.
 663 *arXiv:1909.11522*, 2019.

664 Chris Mingard, Guillermo Valle-Pérez, Joar Skalse, and Ard A Louis. Is SGD a bayesian sampler?
 665 well, almost. *Journal of Machine Learning Research*, 2021.

666 Chris Mingard, Henry Rees, Guillermo Valle-Pérez, and Ard A Louis. Do deep neural networks
 667 have an inbuilt occam's razor? *arXiv:2304.06670*, 2023.

668 Iman Mirzadeh, Keivan Alizadeh, Sachin Mehta, Carlo C Del Mundo, Oncel Tuzel, Golnoosh
 669 Samei, Mohammad Rastegari, and Mehrdad Farajtabar. Relu strikes back: Exploiting activation
 670 sparsity in large language models. *arXiv:2310.04564*, 2023.

671 Tom M Mitchell. The need for biases in learning generalizations. *Rutgers University CS tech report
 672 CBM-TR-117*, 1980.

673 Aaron Mueller and Tal Linzen. How to plant trees in language models: Data and architectural effects
 674 on the emergence of syntactic inductive biases. *Transactions of the ACL*, 2022.

675 Laker Newhouse, R Preston Hess, Franz Cesista, Andrii Zahorodnii, Jeremy Bernstein, and Phillip
 676 Isola. Training transformers with enforced lipschitz constants. *arXiv:2507.13338*, 2025.

677 Yaniv Nikankin, Anja Reusch, Aaron Mueller, and Yonatan Belinkov. Arithmetic without algo-
 678 rithms: Language models solve math with a bag of heuristics. *arXiv:2410.21272*, 2024.

679 Isabel Papadimitriou and Dan Jurafsky. Injecting structural hints: Using language models to study
 680 inductive biases in language learning. In *Proceedings of ACL*, 2022.

681 Guilherme Penedo, Hynek Kydlíček, Anton Lozhkov, Margaret Mitchell, Colin A Raffel, Leandro
 682 Von Werra, Thomas Wolf, et al. The fineweb datasets: Decanting the web for the finest text data
 683 at scale. *NeurIPS*, 2024.

684 Jackson Petty, Sjoerd van Steenkiste, and Tal Linzen. How does code pretraining affect language
 685 model task performance? *arXiv:2409.04556*, 2024.

686 Mohammad Pezeshki, Oumar Kaba, Yoshua Bengio, Aaron C Courville, Doina Precup, and Guil-
 687 laume Lajoie. Gradient starvation: A learning proclivity in neural networks. *NeurIPS*, 2021.

688 Ofir Press, Noah A Smith, and Mike Lewis. Train short, test long: Attention with linear biases
 689 enables input length extrapolation. *arXiv preprint arXiv:2108.12409*, 2021.

690 Aahlad Manas Puli, Lily Zhang, Yoav Wald, and Rajesh Ranganath. Don't blame dataset shift!
 691 shortcut learning due to gradients and cross entropy. *NeurIPS*, 2023.

702 Alec Radford, Jeffrey Wu, Rewon Child, David Luan, Dario Amodei, Ilya Sutskever, et al. Language
 703 models are unsupervised multitask learners. *OpenAI blog*, 2019.

704

705 Nasim Rahaman, Aristide Baratin, Devansh Arpit, Felix Draxler, Min Lin, Fred Hamprecht, Yoshua
 706 Bengio, and Aaron Courville. On the spectral bias of neural networks. In *ICML*. PMLR, 2019.

707

708 Prajit Ramachandran, Barret Zoph, and Quoc V Le. Swish: a self-gated activation function.
arXiv:1710.05941, 2017.

709

710 Prajit Ramachandran, Barret Zoph, and Quoc V. Le. Searching for activation functions. In *ICLR*,
 711 2018.

712 Riccardo Rende, Federica Gerace, Alessandro Laio, and Sebastian Goldt. A distributional simplicity
 713 bias in the learning dynamics of transformers. *NeurIPS*, 37, 2024.

714

715 Vishwanath Saragadam, Daniel LeJeune, Jasper Tan, Guha Balakrishnan, Ashok Veeraraghavan,
 716 and Richard G Baraniuk. Wire: Wavelet implicit neural representations. In *CVPR*, 2023.

717

718 Hemanth Saratchandran, Sameera Ramasinghe, Violetta Shevchenko, Alexander Long, and Si-
 719 mon Lucey. A sampling theory perspective on activations for implicit neural representations.
arXiv:2402.05427, 2024a.

720

721 Hemanth Saratchandran, Jianqiao Zheng, Yiping Ji, Wenbo Zhang, and Simon Lucey. Rethinking
 722 softmax: Self-attention with polynomial activations. *arXiv:2410.18613*, 2024b.

723

724 Simone Scardapane, Steven Van Vaerenbergh, Simone Totaro, and Aurelio Uncini. Kafnets: Kernel-
 725 based non-parametric activation functions for neural networks. *Neural Networks*, 2019.

726

727 Imanol Schlag, Kazuki Irie, and Jürgen Schmidhuber. Linear transformers are secretly fast weight
 728 programmers. In *ICML*. PMLR, 2021.

729

730 Noam Shazeer. Glu variants improve transformer. *arXiv:2002.05202*, 2020.

731

732 Zachary Shinnick, Liangze Jiang, Hemanth Saratchandran, Anton van den Hengel, and Damien
 733 Teney. Transformers pretrained on procedural data contain modular structures for algorithmic
 734 reasoning. *arXiv preprint arXiv:2505.22308*, 2025.

735

736 David So, Wojciech Mańke, Hanxiao Liu, Zihang Dai, Noam Shazeer, and Quoc V Le. Searching
 737 for efficient transformers for language modeling. *NeurIPS*, 34, 2021a.

738

739 David R So, Wojciech Manke, Hanxiao Liu, Zihang Dai, Noam Shazeer, and Quoc V Le. Primer:
 740 Searching for efficient transformers for language modeling, 2022. *arXiv:2109.08668*, 2021b.

741

742 Leon René Sütfeld, Flemming Brieger, Holger Finger, Sonja Füllhase, and Gordon Pipa. Adaptive
 743 blending units: Trainable activation functions for deep neural networks. In *Intelligent Computing:
 744 Proceedings of the Computing Conference*. Springer, 2020.

745

746 Remi Tachet, Mohammad Pezeshki, Samira Shabanian, Aaron Courville, and Yoshua Bengio. On
 747 the learning dynamics of deep neural networks. *arXiv:1809.06848*, 2018.

748

749 Camilo Tamayo-Rousseau, Yunjia Zhao, Yiqun Zhang, and Randall Balestriero. Your attention
 750 matters: to improve model robustness to noise and spurious correlations. *arXiv:2507.20453*,
 2025.

751

752 Yi Tay, Mostafa Dehghani, Samira Abnar, Hyung Won Chung, William Fedus, Jinfeng Rao, Sharan
 753 Narang, Vinh Q Tran, Dani Yogatama, and Donald Metzler. Scaling laws vs model architectures:
 754 How does inductive bias influence scaling? *arXiv:2207.10551*, 2022.

755

Damien Teney, Ehsan Abbasnejad, Simon Lucey, and Anton van den Hengel. Evading the simplicity
 bias: Training a diverse set of models discovers solutions with superior ood generalization.
arXiv:2105.05612, 2021.

Damien Teney, Maxime Peyrard, and Ehsan Abbasnejad. Predicting is not understanding: Recognizing
 and addressing underspecification in machine learning. In *ECCV*. Springer, 2022.

756 Damien Teney, Armand Mihai Nicolicioiu, Valentin Hartmann, and Ehsan Abbasnejad. Neural
 757 redshift: Random networks are not random functions. In *CVPR*, 2024.

758

759 Damien Teney, Liangze Jiang, Florin Gogianu, and Ehsan Abbasnejad. Do we always need the
 760 simplicity bias? looking for optimal inductive biases in the wild. In *CVPR*, 2025.

761 Guillermo Valle-Perez, Chico Q Camargo, and Ard A Louis. Deep learning generalizes because the
 762 parameter-function map is biased towards simple functions. *arXiv:1805.08522*, 2018.

763

764 Bhavya Vasudeva, Deqing Fu, Tianyi Zhou, Elliott Kau, Youqi Huang, and Vatsal Sharan. Simplicity
 765 bias of transformers to learn low sensitivity functions. *arXiv:2403.06925*, 2024.

766

767 Ashish Vaswani, Noam Shazeer, Niki Parmar, Jakob Uszkoreit, Llion Jones, Aidan N Gomez,
 768 Łukasz Kaiser, and Illia Polosukhin. Attention is all you need. *NeurIPS*, 2017.

769

770 Petar Veličković, Christos Periwalopoulos, Federico Barbero, and Razvan Pascanu. softmax is not
 771 enough (for sharp out-of-distribution). *arXiv:2410.01104*, 2024.

772

773 Alex Warstadt and Samuel R Bowman. What artificial neural networks can tell us about human
 774 language acquisition. *Trends in Cognitive Sciences*, 2020.

775

776 Colin White, Mahmoud Safari, Rhea Sukthanker, Binxin Ru, Thomas Elsken, Arber Zela, De-
 777 badeeptha Dey, and Frank Hutter. Neural architecture search: Insights from 1000 papers.
 778 *arXiv:2301.08727*, 2023.

779

780 David H Wolpert. The lack of a priori distinctions between learning algorithms. *Neural computation*,
 781 1996.

782

783 David H Wolpert. The supervised learning no-free-lunch theorems. *Soft computing and industry:
 784 Recent applications*, 2002.

785

786 Zhi-Qin John Xu, Yaoyu Zhang, Tao Luo, Yanyang Xiao, and Zheng Ma. Frequency principle:
 787 Fourier analysis sheds light on deep neural networks. *arXiv:1901.06523*, 2019.

788

789 Xiulin Yang et al. (anything) goes? a crosslinguistic study of (im)possible language learning in lms.
 790 In *Proceedings of ACL*, 2024.

791

792 York Yong. Clean version of the wikipedia. Available at <https://www.kaggle.com/api/v1/datasets/download/yorkyong/text8-zip>, 2025.

793

794 Ailing Zeng, Muxi Chen, Lei Zhang, and Qiang Xu. Are transformers effective for time series
 795 forecasting? In *AAAI*, 2023.

796

797 Zhongwang Zhang, Pengxiao Lin, Zhiwei Wang, Yaoyu Zhang, and Zhi-Qin John Xu. Initial-
 798 ization is critical to whether transformer fits composite function by inference or memorizing.
 799 *arXiv:2405.05409*, 2024.

800

801 Ziqian Zhong and Jacob Andreas. Algorithmic capabilities of random transformers.
 802 *arXiv:2410.04368*, 2024.

803

804 Hattie Zhou, Arwen Bradley, Eta Littwin, Noam Razin, Omid Saremi, Josh Susskind, Samy Bengio,
 805 and Preetum Nakkiran. What algorithms can transformers learn? a study in length generalization.
 806 *arXiv:2310.16028*, 2023.

807

808 Yongchao Zhou, Uri Alon, Xinyun Chen, Xuezhi Wang, Rishabh Agarwal, and Denny Zhou. Trans-
 809 formers can achieve length generalization but not robustly. *arXiv preprint arXiv:2402.09371*,
 2024.

810

811 Barret Zoph and Quoc V. Le. Neural architecture search with reinforcement learning. In *ICLR*,
 812 2017.

813

814

815

816

817

818

819

820

821

822

823

824

825

826

827

828

829

830

831

832

833

834

835

836

837

838

839

840

841

842

843

844

845

846

847

848

849

850

851

852

853

854

855

856

857

858

859

860

861

862

863

864

865

866

867

868

869

870

871

872

873

874

875

876

877

878

879

880

881

882

883

884

885

886

887

888

889

890

891

892

893

894

895

896

897

898

899

900

901

902

903

904

905

906

907

908

909

910

911

912

913

914

915

916

917

918

919

920

921

922

923

924

925

926

927

928

929

930

931

932

933

934

935

936

937

938

939

940

941

942

943

944

945

946

947

948

949

950

951

952

953

954

955

956

957

958

959

960

961

962

963

964

965

966

967

968

969

970

971

972

973

974

975

976

977

978

979

980

981

982

983

984

985

986

987

988

989

990

991

992

993

994

995

996

997

998

999

1000

APPENDIX

A ADDITIONAL RELATED WORK

Inductive biases in deep learning are due to choices of architecture (Goyal & Bengio, 2022) and of the learning algorithm (optimizer, objective, regularizers (Kukačka et al., 2017)). We focus on the former. The simplicity bias has been studied from both aspects. Most explanations attribute it to loss functions (Pezeshki et al., 2021) and gradient descent (Arora et al., 2019; Hermann & Lampinen, 2020; Lyu et al., 2021; Tachet et al., 2018). But work on untrained networks shows that it can be explained with architectures alone (De Palma et al., 2019; Goldblum et al., 2023; Mingard et al., 2019; Teney et al., 2024; Valle-Perez et al., 2018). Teney et al. (2024) showed that the choice of activation function can modulate the simplicity bias. The **spectral bias** (Rahaman et al., 2019; Kalimeris et al., 2019) or frequency principle (Xu et al., 2019) is a related but different effect related to training dynamics: NNs approximate low-frequency components of the target function earlier during training with SGD.

Simplicity bias in transformers. The hypothesis of a simplicity bias in NNs has also been studied specifically in transformers. Hahn et al. (2021) shows that common models in NLP are biased to learn low-sensitivity functions. Bhattacharya et al. (2022) shows that transformers are more biased for simplicity than LSTMs. Dziri et al. (2023) examine large pretrained models and determine that that tend rely on shortcut learning on simple reasoning tasks. Zhou et al. (2023) focus on length generalization and show that transformers learn the shortest program in the RASP language that fits the training data –a specific form of the simplicity bias. Rende et al. (2024) study BERT-like models and find that they learn simple functions first during the course of training. Zhang et al. (2024) find that the scale of initialization can influence a transformer’s learning of a generalizing or memorizing solution. Vasudeva et al. (2024) further study the bias of transformers for learning low-sensitivity functions using the NTK theory. Hahn & Rofin (2024) show that sensitive functions are hard to learn for transformers because they correspond to sharp solutions in their optimization landscape as a side-effect of the simplicity bias.

Activation functions are key for introducing non-linearities in NNs. Many options were considered early on, e.g. sine activations in the Fourier Neural Networks from 1988 (Gallant, 1988). ReLUs are often credited for enabling the rise of deep learning by avoiding vanishing gradients (Maas et al., 2013). However they are also essential in inducing the simplicity bias (Teney et al., 2024) which may be just as important. The research community has slowly converged towards smooth handcrafted variants of ReLUs such as GeLUs (Dubey et al., 2022; Hendrycks & Gimpel, 2016; Ramachandran et al., 2017). Some works proposed **learning activation functions** using extra parameters optimized alongside the weights of the network (Alexandridis et al., 2025; Apicella et al., 2019; 2021; Bingham et al., 2020; Chelly et al., 2024; Ducotterd et al., 2024; Jagtap et al., 2020; Scardapane et al., 2019; Sütfeld et al., 2020). See Jagtap & Karniadakis (2023) for a comprehensive review. The goal is to better fit the training data with an activation function that can evolve during training. In contrast, we use meta learning to find an activation function that induces better inductive biases, such that training with this *fixed* activation provides better generalization. This requires bi-level optimization, episodic training, and unbiased parametrization that allows us to learn activations very different from existing ones. **Kolmogorov-Arnold Networks** (Liu et al., 2024) parametrize the connections in a NN, which is equivalent to learning different activation functions across channels and layers. They use a parametrization as splines similar to ours. Their benefits in physics-related problems likely result from the alterations to the inductive biases studied in this paper. Our method differs from **neural architecture search** (White et al., 2023) in its ability to discover novel activation functions from scratch, rather than selecting from predefined candidates (Sütfeld et al., 2020) or from a narrow set of parametric functions (Alexandridis et al., 2025).

Length generalization refers to the ability of a model to generalize to sequences longer than seen during training, especially for algorithmic tasks (e.g. arithmetic operations on numbers with more digits). This remains a challenge despite extensive work on positional encodings, which only partially address the problem (Anil et al., 2022; Kazemnejad et al., 2023; Zhou et al., 2024). This paper shows that other aspects of the architecture can be important. We use the COPY task as proof of concept and show that different MLP activation functions can bring a significant improvement to the existing Alibi encodings (Press et al., 2021).

864 **Learnability and inductive biases.** The learnability of any given task is a fundamental question
 865 in machine learning. It is well known that inductive biases are indispensable for generalization to
 866 unseen data (Mitchell, 1980) and that no learning algorithm is universally useful, as per one of
 867 the no-free lunch theorems (Wolpert, 2002)). Meanwhile, neural networks have nevertheless proved
 868 widely successful. The broad applicability of transformers, in particular, suggests that their inductive
 869 bias has a broad relevance to real-world data (Goldblum et al., 2023). The **simplicity bias** is a
 870 broad and vague characterization of these properties. Various studies have established however that
 871 the simplicity bias is not universally beneficial (Domingos, 1999; Teney et al., 2025; Zeng et al.,
 872 2023) and even responsible for failure cases such as **shortcut learning** (Geirhos et al., 2020; Puli
 873 et al., 2023; Teney et al., 2021) or the amplification of biases and performance disparities (Bell &
 874 Sagun, 2023). Even the underlying principle supporting the simplicity bias, known as **Occam’s
 875 razor**, has long been debated in the philosophical literature because it lacks a justification from first
 876 principles (Mingard et al., 2023, Appendix A). A prominent argument for simplicity is rooted in
 877 algorithmic information theory (Dingle et al., 2018) with results stating essentially that “*a bias in
 878 the distribution of target functions must be towards low complexity*”. However, this only means that
 879 simplicity is a good prior on average, but not necessarily the best choice for any task or dataset.

880 Studies in linguistics and cognitive science have also examined the question of learnability. This
 881 includes studies on the influence of architectures and data on generalization during **language ac-
 882 quisition**, both for humans and machines (Futrell & Mahowald, 2023; Millière, 2024; Warstadt &
 883 Bowman, 2020). This explains how syntactic and structural biases arise and how they can be con-
 884 trolled (Mueller & Linzen, 2022; Papadimitriou & Jurafsky, 2022; Yang et al., 2024). Our paper
 885 complements this line of work since it helps clarify the impact of architectures on generalization.
 886 Our approach is quite different though. Our method allows searching through the space of archi-
 887 tectures via the optimization of non-linearities. This matters because current popular designs (e.g.
 888 transformers) are contingent on external factors, cf. the **Hardware Lottery** (Hooker, 2021)).

889 **Connection with prior work.** This paper is a follow-up the study by Teney et al. (2025) that
 890 uses trainable non-linearities to study whether the *simplicity bias* of standard neural architectures
 891 is always desirable. It was however limited to MLPs and toy data, and relied on an expensive
 892 optimization method unsuitable to modern architectures. In comparison, our main innovations are:
 893 • a formulation of trainable non-linearities that applies to transformers’ MLPs and attention layers;
 894 • a tractable optimization method replacing the expensive bi-level approach from prior work;
 895 • the study of mainstream domains (language modeling, algorithmic reasoning);
 896 • the study of cross-task compatibility, whereas prior work focuses on individual datasets;
 897 • a demonstration of massive improvements on algorithmic tasks;
 898 • a PyTorch implementation that allows swapping standard activation functions for optimized ones
 899 with a few lines of code, available at <https://github.com/anonymized/anonymized>.

900
 901
 902
 903
 904
 905
 906
 907
 908
 909
 910
 911
 912
 913
 914
 915
 916
 917

918 **B IMPLEMENTATION DETAILS**
919920
921 **Proposed method.** We provide a formal description of our method in Algorithm 1.
922923 **Algorithm 1** Proposed method (stage I) to optimize a transformer architecture for a specific task.
924925 **Input:**
926927 Training data $\mathbb{D} = \{\mathbf{s}_i\}_{i=1}^n$ as token sequences $\mathbf{s} \in \mathbf{S}$.
928 Baseline architecture \mathcal{T} instantiable as next-token prediction model $T_{\theta}: \mathbf{S} \rightarrow \mathbf{S}$ of weights θ .
929 $\mathcal{L}(\cdot, \cdot)$: Loss function. α : Fraction of held-out data. M : Number of parallel models.930 **Method:**
931932 Define a new architecture $\hat{\mathcal{T}}_{\theta_A, \theta_{MLP}}$ by replacing
933 – softmaxes with $\sum_j K(\mathbf{Q}_i, \mathbf{K}_j) \mathbf{V}_j / \sum_j K(\mathbf{Q}_i, \mathbf{K}_j)$, where $K(\mathbf{Q}, \mathbf{K}) = \phi_{\theta_A}(\mathbf{Q})^\top \phi_{\theta_A}(\mathbf{K})$.
934 – GeLUs with a linear spline $\phi_{\theta_{MLP}}$,
935 where architecture hyperparameters θ_A and θ_{MLP} specify the value of splines ϕ at their keypoints.
936 Instantiate M untrained models of architecture $\hat{\mathcal{T}}$ as $\hat{T}_{\theta_1}^1 \dots \hat{T}_{\theta_M}^M$.
937 Split \mathbb{D} into \mathbb{D}_{arch} and \mathbb{D}_{wts} of sizes αn and $(1-\alpha)n$.938 **while** not converged **SGD training loop** —939 Sample mini-batch \mathbb{D}^0 from \mathbb{D}_{arch} and $\mathbb{D}^1 \dots \mathbb{D}^M$ from \mathbb{D}_{wts}
940 Eval. loss of each individual model on its own data \mathbb{D}^m : $L_{\text{wts}}^m \leftarrow \sum_{\mathbf{s} \in \mathbb{D}^m} \mathcal{L}(\hat{T}_{\theta_m}^m(\mathbf{s}), \mathbf{s})$
941 Eval. combined loss of all models together on \mathbb{D}^0 : $L_{\text{arch}} \leftarrow \sum_m \sum_{\mathbf{s} \in \mathbb{D}^0} \mathcal{L}(\hat{T}_{\theta_m}^m(\mathbf{s}), \mathbf{s})$
942 Update weights of each model: $\forall m, \theta_m \leftarrow \text{SGD}(\theta_m, \nabla_{\theta} L_{\text{wts}}^m)$
943 Update architecture: $(\theta_A, \theta_{MLP}) \leftarrow \text{SGD}((\theta_A, \theta_{MLP}), \nabla_{(\theta_A, \theta_{MLP})} L_{\text{arch}})$ 944 $(\theta_A^*, \theta_{MLP}^*) \leftarrow (\theta_A, \theta_{MLP})$.
945946 **Output:** optimized architecture $\hat{\mathcal{T}}_{\theta_A^*, \theta_{MLP}^*}$
947 Now $\hat{\mathcal{T}}$ can be used like any other architecture, treating θ_A^* and θ_{MLP}^* as fixed hyperparameters.948
949 **Baseline transformer architecture.** Our baseline is a GPT-2-style architecture (Radford et al.,
950 2019). It uses standard multi-head attention, GeLU activation functions in the MLPs, post-norm
951 layers, learned absolute positional embeddings, and a width multiplier of 4 in the MLP hidden
952 layers. All weights are initialized from Gaussians of standard deviation 0.02 truncated at 2 standard
953 deviations.
954955 **Parametrization of non-linearities as linear splines.** We want a search space free of priors such
956 as the smoothness and monotonicity enforced in similar work on the learning of activation functions
957 (e.g. Apicella et al. (2019); Chelly et al. (2024)). We therefore choose to learn a non-linearity as
958 a linear spline $\phi_{\theta}: \mathbb{R} \rightarrow \mathbb{R}$ with control points defined by θ . We define n_c points spread regularly
959 in an interval $[a, b]$, typically $n_c = 122$ points in $[-20, +20]$ for a spacing of $1/3$ between points
960 (see hyperparameters in Table 4). Then ϕ represents piecewise linear segments interpolating values
961 specified in the learned parameters $\theta := [\phi_{\theta}(a), \dots, \phi_{\theta}(b)] \in \mathbb{R}^{n_c}$. The function ϕ can represent
962 simple and complex functions, including smooth curves, periodic functions, sharp transitions, etc.963 **Datasets for algorithmic tasks.** For most tasks, we generated data with code adapted from Zhong
964 & Andreas (2024): https://github.com/fjzzq2002/random_transformers. While
965 this prior work generates some of the data on-the-fly, we pre-generate all the data to ensure that the
966 training/validation/test splits are strictly disjoint.967 For MANO, we re-implemented the data generation based on the description by Allen-Zhu (2025).
968 Compared to this prior work, we scaled down the task to allow using smaller models. We generated
969 1e5 training examples, with a number of operations in each sequence in [1,3], a modulus of 7, and
970 without tokens signaling the number of operations.

971 For all algorithmic tasks, we use a test set of 1e3 examples, strictly disjoint from the training set.

972 **Datasets for language modeling.** For datasets tokenized at the character level, every character or
 973 symbol in the data simply corresponds to one token. For the TINYSTORIES, SHAKESPEARE, and
 974 ENWIK8 datasets tokenized at the subword level, we use the byte-pair encoding (BPE, Gage (1994))
 975 tokenizer from GPT-2 Radford et al. (2019). We consider it a consistent choice suitable to our
 976 different datasets since it was originally trained on very diverse data. For the CODESEARCHNET
 977 datasets, we use the tokenizer of the CodeGPT model (CodeGPT, 2024). For each dataset, we
 978 discard tokens with fewer than 200 training occurrences. This significantly reduces the vocabulary
 979 size and training costs. This should not undermine the results of our experiments: if anything,
 980 including more rare tokens could reveal larger differences across datasets.

981 **Metrics.** For the algorithmic tasks, we measure performance as the token-wise accuracy of the “out-
 982 put” part of the generated sequences (the same part of the sequences as used to compute the training
 983 loss). This allows a finer-grained evaluation of partial success than the sequence-wise accuracy.

984 For the COPY task, we use the sequence-wise accuracy because the token-wise accuracy can remain
 985 falsely high when a model fails at length generalization.

987 For the language modeling tasks, we measure performance using the training perplexity (exponential
 988 of cross-entropy loss) as well as token-wise accuracy on validation data as a more intuitive measure
 989 of performance. For the accuracy, we measure it on the latter half of the context window to ensure
 990 that we evaluate predictions with enough conditioning.

991 For the compatibility across algorithmic tasks (Figure 5), we plot the difference in test accuracy
 992 with the baseline after a fixed number of steps. We adapt the number of steps to each task to capture
 993 improvements in generalization and/or training speed depending on the task. This is because both
 994 the baseline and optimized architectures saturate at perfect accuracy for multiple tasks, hence the
 995 *final* accuracy alone is not informative.

- 996 • MEMORIZ: 150 steps.
- 997 • PARENTHESES: 300 steps.
- 998 • ADDMOD: 300 steps.
- 999 • HAYSTACK: 400 steps.
- 1000 • ADD: 700 steps.
- 1001 • ADDREVERSED: 350 steps.
- 1002 • COPY: 2,000 steps.
- 1003 • MANO: 3,000 steps.

1004 **Hyperparameters.** We tuned the hyperparameters in Table 4 for a standard transformer on each
 1005 task, to make sure that our optimized architectures are compared against strong baselines. For
 1006 example, we use the Canon layers proposed by Allen-Zhu (2025) for many tasks (sequence-wise 1D
 1007 convolutions) because they clearly improve the performance of the baseline.

1008 Table 4: Hyperparameters used for each task.

	MEMORIZ	PARENTHESES	ADDMOD	HAYSTACK	ADD	ADDREVERSED	COPY	MANO	Language datasets
Num. layers				2				4	
Num. att. heads	2	2	2	2	2	2	2	8	4
Width	32	32	32	128	128	128	128	128	512
Tied embeddings				No				Yes	
Canon layers				No				Yes	
Num. tr. steps	500	500	1,000	1,000	1,000	1,000	2,000	5,000	3,000
Peak LR	.005	.001	.02	.001	.001	.001	.004	.001	.001
Batch size			512					64	
Optimizer				Adam					
Adam (β_1, β_2)			(0.9, 0.999)			(0.92, 0.98)		(0.9, 0.999)	
LR schedule			5% linear warm-up, 50% cosine cool-down (not necessary for algorithmic tasks; used on all tasks for consistency)						
Weight decay			0 (better on all tasks than using any weight decay)						
Dropout rate			0						
Parallel models M			8				3		
Spline range $[a, b]$				[-20, 20]					
Spline spacing n_c			1/9				1/3		

1026 C ADDITIONAL RESULTS ON ALGORITHMIC TASKS
1027

1028 **Training curves.** Figure 10 shows that the optimized architectures (2nd and 3rd columns) always
1029 converge significantly faster than a baseline transformer (1st column) and show less variance across
1030 seeds. There is little difference between the 2nd and 3rd columns, which means that most of the
1031 benefits come from optimizing the non-linearity within the MLP layers rather than the attention.
1032

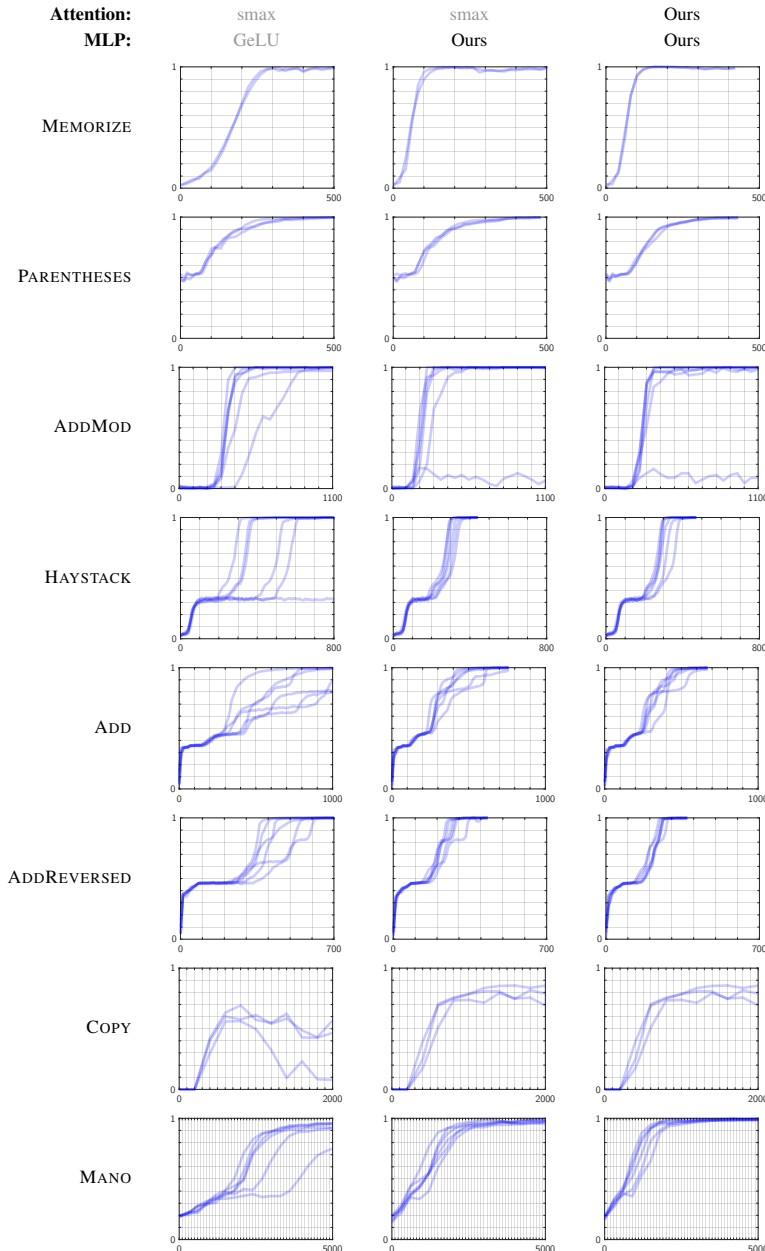
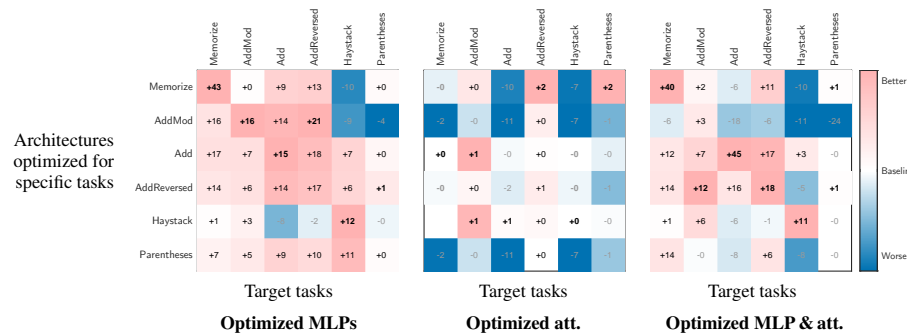


Figure 10: Training curves (test accuracy vs. training steps, one curve per seed) of models trained on algorithmic tasks with a baseline transformer (first column) or optimized architectures (second and third columns).

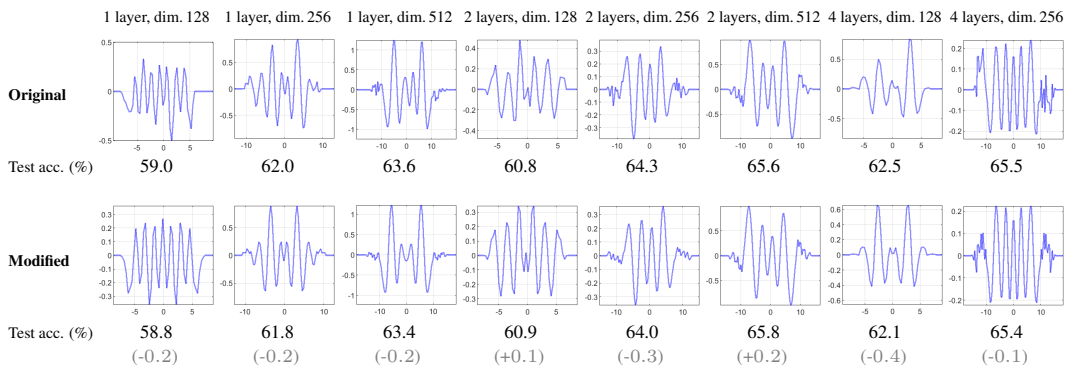
1080
 1081 **Compatibility of architectures across algorithmic tasks.** We present below the full results fol-
 1082 lowing the format of Figure 5. We show the effect when optimizing the non-linearities in MLP or
 1083 attention layers, or both. Optimizing the non-linearities in the attention proves to be really challeng-
 1084 ing, and the best results are usually obtained by optimizing only the MLPs.
 1085



1091
 1092
 1093
 1094
 1095
 1096 Figure 11: Compatibility of architectures across algorithmic tasks (difference in test accuracy with
 1097 the baseline after a fixed number of steps).
 1098
 1099
 1100
 1101
 1102
 1103
 1104
 1105
 1106
 1107
 1108
 1109
 1110
 1111
 1112
 1113
 1114
 1115
 1116
 1117
 1118
 1119
 1120
 1121
 1122
 1123
 1124
 1125
 1126
 1127
 1128
 1129
 1130
 1131
 1132
 1133

1134 **D ADDITIONAL RESULTS ON LANGUAGE MODELING**
1135

1136 **Manipulating optimized non-linearities.** In these experiments, we slightly modify the optimized
1137 MLP non-linearities to understand the importance of their fine details. Since they often look like
1138 sinusoidal wavelets, perhaps an even more regular version of them could perform better. We auto-
1139 mate a “cleaning” process of the optimized non-linearities as follows. We take the optimized spline,
1140 reverse it along the X and/or Y axis (yielding three different versions), then align it with the original
1141 one by maximizing their cross-correlation. We then keep the average of the two. Among the three
1142 versions, we retain the one with the highest cross-correlation (i.e. similarity) with the original spline.
1143 The result is symmetric or anti-symmetric with fewer irregularities than the original one. We visual-
1144 ize this effect in Figure 12 on MLP non-linearities optimized for TINYSTORIES and various model
1145 sizes. We train models with these, but in almost every case, they perform worse than the original
1146 ones. This shows that fine details in the original optimized non-linearities matter.

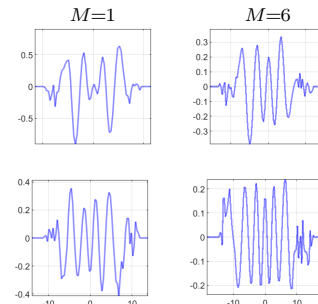


1159 Figure 12: MLP non-linearities optimized for TINYSTORIES and versions modified to enforce sym-
1160 metry. Almost all of these perform worse than the original ones, whose fine details therefore matter.
1161

1162 **Multi-model training.** We compare in Table 5 architectures for TINYSTORIES obtained with the
1163 proposed method and $M = 1$ or $M = 6$ models in parallel. The latter are slightly better, and the
1164 optimized non-linearities look slightly more regular.
1165

1166 Table 5: Models for TINYSTORIES with architectures optimized with $M=1$ or 6 parallel models.
1167

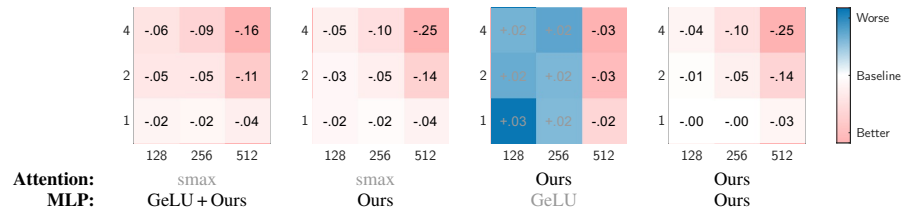
(Models with 2 layers, width 256)	Attention MLP	smax Linear	smax GeLU	smax Ours, $M=1$	smax Ours, $M=6$
	Tr. perplexity	1.78	1.58	1.59	1.57
(Models with 4 layers, width 256)	Val. acc. (%)	59.9	63.7	63.8	64.3
	Attention MLP	smax Linear	smax GeLU	smax Ours, $N=1$	smax Ours, $N=6$
	Tr. perplexity	1.73	1.53	1.53	1.52
	Val. acc. (%)	60.8	65.1	65.3	65.4



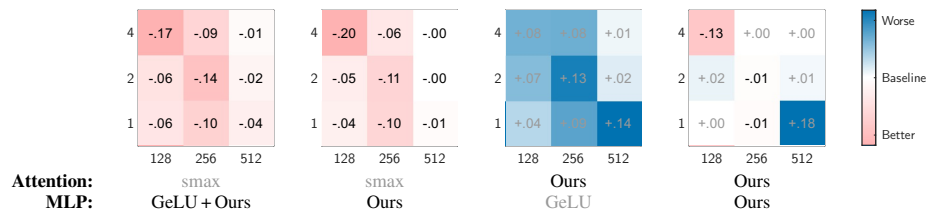
1178 **Existing methods.** Below are references for the attention and MLP designs evaluated in Table 3.
1179

- 1180 • **Adaptive softmax:** Veličković et al. (2024).
- 1181 • **NormSoftmax:** Jiang et al. (2023).
- 1182 • **Polynomial attention P1:** $(\mathbf{Q}^\top \mathbf{K}) / \sqrt{\text{seqLength}}$: Saratchandran et al. (2024b).
- 1183 • **Polynomial attention P3:** $(\mathbf{Q}^\top \mathbf{K})^3 / \sqrt{\text{seqLength}}$: Saratchandran et al. (2024b).
- 1184 • **GLU:** Shazeer (2020).
- 1185 • **ReLU²:** So et al. (2021b).
- 1186 • **Sinc:** Saratchandran et al. (2024a).
- 1187 • **Gaussian:** Saragadam et al. (2023).

1188
 1189 **Full results on Shakespeare.** We present below results on the SHAKESPEARE dataset for various
 1190 model sizes, in the same format as Figure 7. The best configuration is to optimize the MLP non-
 1191 linearities while keeping the original softmax attention (second panels from the left).
 1192

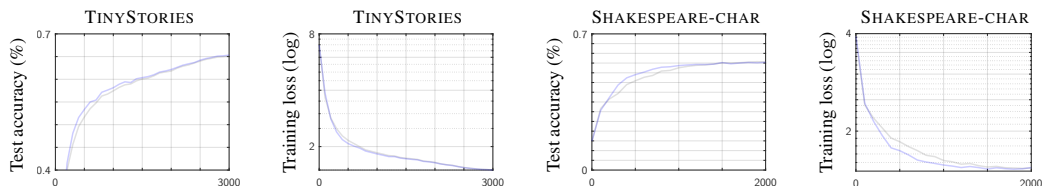


1200 Figure 13: Absolute improvements in training perplexity on character-level SHAKESPEARE for
 1201 models of different sizes (number of layers \times width).
 1202



1211 Figure 14: Same as Figure 13 with subword-level tokenization.
 1212

1213 **Training curves on language datasets.** Figure 15 shows that the optimized architectures (■) show
 1214 a larger improvement over a baseline transformer early during training, which then diminishes.
 1215



1222 Figure 15: Training curves on language datasets with baseline (■) and optimized (■) architectures.
 1223

1242 E RESULTS WITH LARGER LANGUAGE MODELS

1244 On the suggestions of reviewers, we perform additional experiments to evaluate the improvements
 1245 from the optimized non-linearities at various scales. We repeat experiments on language modeling
 1246 as in Section 4 with the following differences.

- 1247 • We use the **FINEWEB dataset** (Penedo et al., 2024), a popular high-quality dataset of cleaned
 1248 and deduplicated English text from CommonCrawl.
- 1249 • We implement our method on top of a very strong baseline, the **NanoGPT Speedrun** (Jordan
 1250 et al., 2024). This is a competitive repository where contributors specifically push the implemen-
 1251 tation and data efficiency of the model on the FINEWEB dataset. We specifically build on top of
 1252 record #16, which includes rotary embeddings, QK normalization, the Muon optimizer, sliding-
 1253 window attention, mixed-precision training, etc. The code was designed for 8 H100 GPUs but
 1254 we adapted it to enable experiments with a single Nvidia RTX 4090 laptop GPU. Our results are
 1255 therefore not directly comparable with the official Speedrun competition. See our code for details:
 1256 <https://github.com/anonymized/anonymized>.
- 1257 • We first run stage I of our method to optimize the MLP non-linearities of a small model, since this
 1258 stage is computationally more expensive (2 layers, width 256, 4 attention heads). We then re-use
 1259 the optimized non-linearity to run stage II (i.e. standard training) with models of **various sizes**
 1260 **from 2 to 12 layers**. This setup therefore evaluates how the optimized non-linearities transfer
 1261 across models of different depths.
- 1262 • We train similar models (with 2 to 12 layers) with a ReLU, which is the best baseline for this
 1263 codebase. We always use a standard attention with a softmax since we found in Section 4 that it
 1264 was difficult to improve upon.

1265 **Results.** The results in Table 6 show that our optimized non-linearities perform similarly or better
 1266 than the baselines. There is little improvement at the smallest scale (probably because the model
 1267 is very weak overall) but we get a consistent improvements at all other scales up to 12 layers,
 1268 surpassing both the ReLU and GeLU baselines in most cases.

1269 Regarding the computational cost of the optimized non-linearities, our implementation (Listing 1)
 1270 is as fast or faster than a ReLU in very small models. In larger models however, they become much
 1271 more expensive. We propose in Appendix F a polynomial approximation. Table 6 shows that this
 1272 approximation performs about as well as the original spline and about as fast as a ReLU.

1274 Table 6: Evaluation of models of various depths trained on FINEWEB (average over 3 seeds).

	Number of layers	2	4	8	10	12
	Number of parameters (M)	91	105	133	148	162
Validation loss (FINEWEB)	Linear	4.21	4.05	3.93	3.90	3.88
	ReLU	4.01	3.87	3.78	3.75	3.73
	GeLU	4.00	3.89	3.72	3.75	3.72
	Ours: linear spline	4.00	3.82	3.72	3.68	3.69
Training time (sec)	Ours: polynomial approx. ($n = 18$)	4.01	3.82	3.72	3.70	3.68
	Number of layers	2	4	8	10	12
	Linear	1,440	1,920	2,940	3,540	19,680
	ReLU	1,500	1,980	3,120	13,080	28,020
	GeLU	1,440	1,920	3,090	20,580	34,020
	Ours: linear spline	1,500	2,070	8,520	26,700	81,720
	Ours: polynomial approx. ($n = 18$)	1,440	2,040	3,180	14,070	29,100

1296 F EFFICIENT IMPLEMENTATION OF SPLINES

1298 **Exact implementation.** Our non-linearities are parametrized as linear splines. We first provide an
 1299 exact efficient implementation (Listing 1) that we find to be as fast as standard activations such as
 1300 GeLUs for small models. However, depending on the architecture and GPU used, this function can
 1301 quickly get bandwidth-constrained and become significantly slower. Therefore we propose a faster
 1302 approximation with polynomials to be used when the spline has already been optimized and is used
 1303 as a frozen non-linearity (i.e. for standard training, as in stage II of our experiments).

```
1304 # Evaluate, at points x (typically in bfloat16), a 1D function defined as the
1305 # linear interpolation of knots, of coordinates 'knotPos' and values 'knotVals',
1306 # (both typically in float32).
1307 @torch.compile(dynamic=False)
1308 def eval_spline(x, knotPos, knotVals):
1309     idx = torch.bucketize(x, knotPos) - 1 # Find the interval each x falls into
1310     idx = idx.clamp(0, len(knotPos) - 2)
1311
1312     stepSize = knotPos[1] - knotPos[0]
1313     x0 = knotPos[0] + idx * stepSize
1314     frac = (x - x0) / stepSize
1315     frac = frac.clamp(0.0, 1.0) # Constant extrapolation beyond the knots
1316
1317     y0 = knotVals[idx]
1318     y1 = knotVals[idx + 1]
1319     out = y0 + frac * (y1 - y0) # Linear interpolation
1320
1321     return out.to(x.dtype) # Back to bfloat16; knotPos/frac/out were float32
```

1316 Listing 1: Exact evaluation of a linear spline, used for stages I and II of most of our experiments.

1318 **Approximation with polynomials.** The splines learned in our experiments with language models
 1319 are quite smooth (unlike with algorithmic tasks in Section 3). It is therefore reasonable to approx-
 1320 imate them with polynomials, which are much simpler and faster to evaluate. Concretely, given a
 1321 linear spline optimized in stage I of our method, we determine an approximation through a least-
 1322 squares fit of a polynomial of chosen degree n on the spline values at its knots, on its support that
 1323 has non-zero values. We choose a high degree ($n = 18$ typically) to ensure high fidelity with the
 1324 original spline and to avoid ringing artifacts near the support boundaries. Beyond the boundaries,
 1325 the polynomial is clamped to 0. For efficiency, we evaluate the polynomial with Horner’s method,
 1326 and implement it in a compiled function using TorchScript (see Listing 2).

```
1327 @torch.jit.script
1328 def eval_polynomial(x: torch.Tensor) -> torch.Tensor:
1329     x = x.clamp(-79.52, 71.65) # Clamp for constant extrapolation
1330     x = x / 79.52 # Normalize to get values within [-1,1] for numerical stability
1331     return (((((((((((((29327.20)*x + 18324.92)*x - 41591.43)*x - 12376.90)*x -
1332     14822.88)*x - 29015.27)*x + 33452.63)*x + 10354.57)*x + 21105.54)*x + 45592.25)*x -
1333     47565.33)*x - 47925.56)*x + 26296.37)*x + 18216.14)*x - 6145.61)*x - 2660.53)*x +
1334     522.13)*x + 66.86)*x - 0.63 # Evaluate polynomial with Horner's method
```

1333 Listing 2: Example of polynomial approximation of a spline (best one from Table 7). It uses Horner’s
 1334 method with hard-coded coefficients and is compiled with TorchScript for efficiency.

1336 **Importance of high degree polynomials.** We tried reducing the maximum degree of the poly-
 1337 nomials. This creates smoother functions that look appealing, but they perform systematically worse
 1338 than high-degree polynomials or than the original spline. This shows the importance of fine details
 1339 in the optimized splines. We also tried to suppress noise and artifacts near the support boundaries,
 1340 by analytically enforcing null derivatives (up to 4th derivatives) of the polynomial at the boundaries.
 1341 The functions are again visually appealing but they do not necessarily work better when training
 1342 models with them. The data-driven optimization is clearly superior to our hand-crafted tweaks. One
 1343 possible improvement that we have not implemented is an approximation with Chebyshev poly-
 1344 nomials. These are known to provide better approximations of functions with finite supports, with less
 1345 artifacts and better numerical stability.

1346 **Do we need splines at all?** We tried to do away with splines entirely and directly optimize coeffi-
 1347 cients of a polynomial in stage I of our method. This completely fails however. Even though splines
 1348 and polynomials can represent similar sets of functions, the different parametrization apply different
 1349 inductive biases on the learned non-linearities. As discussed in Section 2, splines are particularly
 effective because they correspond to the most uniform prior on the space of functions.

1350
 1351 **Evaluation of polynomial approximations.** We train small language models on FINEWEB with
 1352 a different non-linearity for the MLP layers. We keep all hyperparameters identical and similar to
 1353 Section E. Here, we use 6 layers, a width of 256, 4 attention heads, $\sim 20M$ parameters, and $\sim 80M$
 1354 training tokens. The results in Table 7 show that our spline performs best and slightly better than a
 1355 ReLU. As expected, **the polynomial approximations are increasingly effective as we increase the**
 1356 **degree.** The approximation then becomes very close to the exact spline. Low-degree polynomials
 1357 yield smoother functions that are visually appealing but do not work as well. This shows that the
 1358 parametrization as a spline is important to capture subtle important details.

1358 Table 7: Models trained on FINEWEB with various MLP non-linearities. Our optimized spline
 1359 works best. Approximations with high-degree polynomials are effective as they faithfully approxi-
 1360 mate the spline.

